Bubble size–topology correlations in two-dimensional foams derived from surface energy minimization

2003 J. Phys. A: Math. Gen. 36 5161

(http://iopscience.iop.org/0305-4470/36/19/301)

INSTITUTE OF PHYSICS PUBLISHING JOURNAL OF PHYSICS A: MATHEMATICAL AND GENERAL

J. Phys. A: Math. Gen. **36** (2003) 5161–5173 PII: S0305-4470(03)57865-9

Bubble size–topology correlations in two-dimensional foams derived from surface energy minimization

M A Fortes[1] **and P I C Teixeira**[1,2]

[1] Departamento de Engenharia de Materiais and Instituto de Ciência e Engenharia de Materiais e Superfícies, Instituto Superior Técnico, Avenida Rovisco Pais, P-1049-001 Lisbon, Portugal
[2] Faculdade de Engenharia, Universidade Católica Portuguesa, Estrada de Talaíde, P-2635-631 Rio de Mouro, Portugal

Received 23 December 2002
Published 29 April 2003
Online at stacks.iop.org/JPhysA/36/5161

Abstract

We obtain the number fractions x_i, the average areas $\langle A\rangle_i$ and the average perimeters $\langle P\rangle_i$ of i-sided bubbles in a two-dimensional foam by minimizing the total surface energy and assuming a simple relation between $\langle P\rangle_i$ and $\langle\sqrt{A}\rangle_i$. Calculations for linear and Weibull distributions of the square root of the bubble area yield large deviations, particularly at small i, from Lewis's and Desch's laws, which linearly relate $\langle A\rangle_i$ and $\langle P\rangle_i$, respectively, to i. Nevertheless, we find good agreement with experimental results for x_i, $\langle P\rangle_i$ and $\langle A\rangle_i$ in foams.

PACS numbers: 83.80.Iz, 82.70.Rr

1. Introduction

Lewis's law [1–4] states that the average area $\langle A\rangle_i$ of i-sided cells in a 'random' partition of the plane into 3-connected cells ($\langle i\rangle = 6$, $i \geqslant 3$, where the angular brackets denote an average over all cells) increases linearly with i:

$$\langle A\rangle_i = \langle A\rangle[1 + c(i - 6)] \tag{1}$$

where $\langle A\rangle \equiv \langle A\rangle_6$ is the average cell area and c is a constant. This law holds approximately for a variety of two-dimensional (2D) (3-connected) networks and for planar sections of three-dimensional (3D) (4-connected) networks, including liquid foams [5–8], polycrystals [9–11], biological tissues [1–4, 12–14], Voronoi tesselations of assemblies of discs moving on an air table [15, 16], pre-mixed flame cells [17], surface-aggregated polyelectrolyte micelles [18], low-density microcellular materials [19] and Bénard–Marangoni convection cells [20]. Although large deviations are frequently found, particularly at low i [6, 7, 15], the law is exact for particular 2D networks [21]. An alternative approximate law has been proposed which in some cases gives better results: this relates the average perimeter $\langle P\rangle_i$ of i-sided cells linearly to i:

$$\langle P\rangle_i = \langle P\rangle[1 + c'(i - 6)] \tag{2}$$

0305-4470/03/195161+13$30.00

where $\langle P\rangle \equiv \langle P\rangle_6$ is the average perimeter and c' is a constant. Equation (2) has been referred to in the literature as Desch's law [22, 23] (or, less commonly, as Feltham's law [8, 24]); recently it was found to describe the length of cracks produced by thermal shock in ceramic tableware [25]. Interestingly, for some non-equilibrium systems such as galactic bubbles near supernova 1987A [26] and patterned breath figures [27], *both* Lewis' and Desch's laws seem to hold approximately. The best-fit coefficients c and c' in equations (1) and (2), respectively, take values in a narrow range for the different networks analysed, usually between 0.10 and 0.30. These laws are to be regarded as empirical, although they can be rationalized on the basis of the minimum entropy principle [28] (but see [29]). In addition, there have been a few attempts to derive Lewis's law in the context of Voronoi networks [16, 30, 31] or of a random neighbour model [32].

Broadly speaking, either law states that cells with many sides tend to be larger, and cells with few sides tend to be smaller. Since cells of small i tend to be surrounded by cells of large i and vice versa (Aboav–Weaire law [33–35]), it follows that small cells tend to be surrounded by large cells and vice versa.

In this paper we investigate the correlation between bubble areas and perimeters and number of bubble sides in 2D dry foams, and derive equations for $\langle A\rangle_i$ and $\langle P\rangle_i$ of i-sided bubbles (where $n \leqslant i \leqslant N$) by requiring that the total energy (i.e. the total film perimeter in a dry foam) be minimized for a given distribution of bubble areas $p(A)$ (section 3). We also determine the number fractions of i-sided bubbles, x_i. The resulting relations depend on $p(A)$ and also on the assumed form of the ratio $e_i = \langle P\rangle_i/\langle\sqrt{A}\rangle_i$ between the average perimeter and the average square root of area of i-sided bubbles. Taking e_i as for regular bubbles (i.e. bubbles whose sides are identical circular arcs, meeting internally at 120°), we have tested the applicability of both Lewis's and Desch's laws for a linear and a Weibull [36] distribution of the square root of the bubble area; the former because of its simplicity, the latter because it is a good representation of experimental results.

This paper is organized as follows: in section 2 we formulate the problem and define the key quantities in our study. Then in section 3 we effect the minimization of the surface energy. Our results for the two particular bubble area distributions mentioned above are presented in section 4. Finally, section 5 summarizes our findings.

2. Formulation of the problem

It is convenient to introduce the variable $a \equiv \sqrt{A}$ and use, instead of the distribution of areas $p(A)$, the distribution $f(a)$ of a. They are related by

$$f(a) = 2\sqrt{A}\,p(A) \qquad p(A) = \frac{f(a)}{2a}. \tag{3}$$

The minimum and maximum values of a are denoted by a_n and a_{N+1}, respectively, where n and N are the minimum and maximum numbers of bubble sides ($n \leqslant i \leqslant N$). We assume that the ratio $e_i = \langle P\rangle_i/\langle\sqrt{A}\rangle_i$ decreases with increasing i, as is the case for regular bubbles [37]. Our aim is to minimize the perimeter for given $f(a)$ and given n and N. We therefore associate smaller areas with bubbles with fewer sides and vice versa; $\langle A\rangle_i$ and $\langle P\rangle_i$ are therefore increasing functions of i (cf equations (1) and (2)). To make the problem tractable, we assume that the minimum perimeter is attained when all i-sided bubbles have a in some range $[a_i, a_{i+1}]$ such that $a_{i+1} > a_i$, for all i, so there are no bubbles with other than i sides in $[a_i, a_{i+1}]$. The whole range $[a_n, a_{N+1}]$ of a thus divides into sub-ranges, each of which contains bubbles all with the same number of sides i, as shown schematically in figure 1. This is obviously an approximation, as in a real foam the sub-ranges may overlap: a bubble with j sides can be smaller than another with $k < j$ sides.

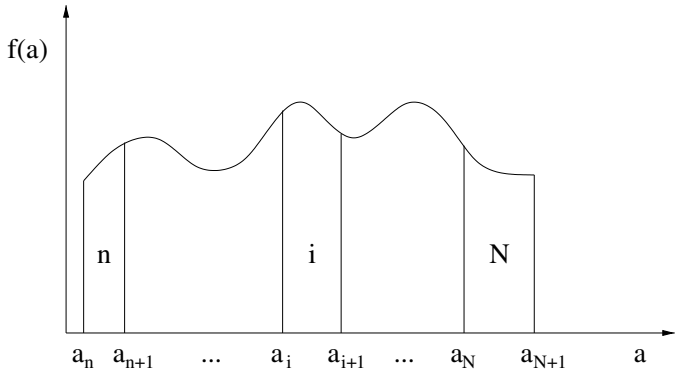

Figure 1. The full range $[a_n, a_{N+1}]$ of $a \equiv \sqrt{A}$ is divided into intervals $[a_i, a_{i+1}]$ such that all cells with a in the ith interval have i sides ($n \leqslant i \leqslant N$). The extrema, a_n and a_{N+1} ($a_n \leqslant a \leqslant a_{N+1}$), are given: all other a_i are determined by perimeter minimization. The distribution $f(a)$ (represented schematically) is the probability density of a.

We shall not be concerned here with the actual space-filling geometry or topology of the foam, except for the requirement that $\langle i \rangle = 6$ (trivalent networks), whence it follows that $n \leqslant 6$ and $N \geqslant 6$. Moreover, we require that there should be both n- and N-sided bubbles, but there may be no bubbles with some intermediate numbers of sides.

For a given $f(a)$, the fraction of x_i of i-sided bubbles (i.e. which have $a \in [a_i, a_{i+1}]$) is

$$x_i = \int_{a_i}^{a_{i+1}} f(a)\,\mathrm{d}a \qquad \sum_{i=1}^{N} x_i = 1 \tag{4}$$

with

$$\langle i \rangle = \sum_{i=1}^{N} i x_i = 6. \tag{5}$$

The average square-root area of i-sided bubbles is then

$$\langle a \rangle_i = \langle \sqrt{A} \rangle_i = \frac{1}{x_i} \int_{a_i}^{a_{i+1}} a f(a)\,\mathrm{d}a \tag{6}$$

and their average area is

$$\langle A \rangle_i = \frac{1}{x_i} \int_{a_i}^{a_{i+1}} a^2 f(a)\,\mathrm{d}a. \tag{7}$$

We assume that the average perimeter $\langle P \rangle_i$ of i-sided cells is related to their average square-root area $\langle a \rangle_i$ by

$$\langle P \rangle_i = e_i \langle a \rangle_i \tag{8}$$

which is of the same form as for regular bubbles [37]; e_i is a weakly decreasing function of i only, see figure 2.

We consider a foam composed of a large number $\mathcal{N}$ of bubbles and treat it as unbounded. The total perimeter of the $\mathcal{N}$ bubbles is

$$P_{\mathrm{tot}} = \frac{1}{2} \sum_{i=n}^{N} \mathcal{N}_i \langle P \rangle_i \tag{9}$$

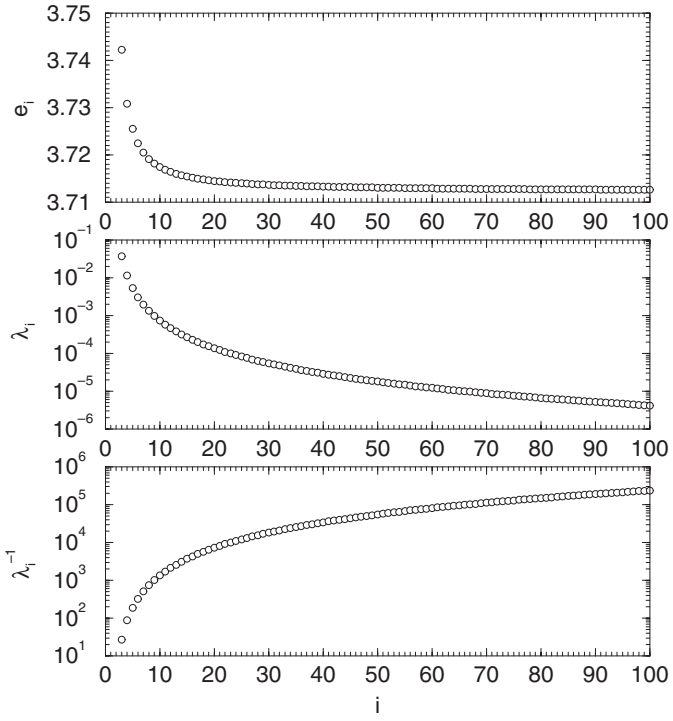

Figure 2. From top to bottom: e_i, λ_i and $1/\lambda_i$ versus i for regular bubbles ($i \geqslant 3$).

where $\mathcal{N}_i$ is the number of i-sided bubbles, and the factor $1/2$ comes from the fact that each film is shared between two bubbles. Combining equations (8) and (9) yields, for the perimeter per bubble,

$$\bar{P} \equiv \frac{P_{\mathrm{tot}}}{\mathcal{N}} = \frac{1}{2}\sum_{i=n}^{N} e_i x_i \langle a \rangle_i . \tag{10}$$

For given $f(a)$, n and N, we need to find the a_i that minimize $\bar{P}$ while satisfying equation (5). We then use these to calculate x_i, $\langle A \rangle_i$ and $\langle P \rangle_i$ as functions of i, in order to test Lewis's and Desch's laws.

3. Perimeter minimization

Here it is shown how the perimeter minimization problem formulated in the preceding section can be solved. We start by using equation (5) to express one of the a_i, say a_N, as a function of the remaining a_i ($i \neq N$):

$$a = a(a_{n+1}, \ldots, a_{N-1}) \tag{11}$$

and then impose the minimum condition on $\bar{P}(a_{n+1}, \ldots, a_{N-1})$:

$$\frac{\partial \bar{P}}{\partial a_i} = 0 \qquad (i = n+1, \ldots, N-1). \tag{12}$$

This has been checked *a posteriori* indeed to yield a minimum (and not a maximum).

For given $f(a)$ (and a_n and a_{N+1}) we define the cumulative density

$$G(a) = \int_{a_n}^{a} f(a')\,\mathrm{d}a' \tag{13}$$

and

$$H(a) = \int_{a_n}^{a} a' f(a')\,\mathrm{d}a'. \tag{14}$$

Furthermore, we introduce the notation

$$G_i \equiv G(a_i) \qquad H_i \equiv H(a_i) \tag{15}$$

for i between n and $N+1$. We have

$$G_n = H_n = 0 \tag{16}$$

$$G_{N+1} = 1 \qquad H_{N+1} = \langle a \rangle \tag{17}$$

$$\frac{\mathrm{d}G_i}{\mathrm{d}a_i} = f(a_i) \qquad \frac{\mathrm{d}H_i}{\mathrm{d}a_i} = a_i f(a_i) \tag{18}$$

and, from equations (4) and (6),

$$x_i = G_{i+1} - G_i \tag{19}$$

$$x_i \langle a \rangle_i = H_{i+1} - H_i. \tag{20}$$

Combining equations (5) and (10), respectively, with equations (4), (13) and (14) yields

$$6 = \sum_{i=n}^{N} i(G_{i+1} - G_i) \tag{21}$$

$$2\bar{P} = \sum_{i=n}^{N} e_i(H_{i+1} - H_i) \tag{22}$$

which, upon rearrangement, become

$$N - 6 = \sum_{i=n+1}^{N} G_i \tag{23}$$

$$2\bar{P} = \sum_{i=n+1}^{N} \lambda_i H_i + e_N \langle a \rangle \tag{24}$$

where we have introduced

$$\lambda_i = e_{i-1} - e_i > 0. \tag{25}$$

We next solve equation (23) for a_N, as a function of the remaining a_i $(n+1 \leqslant i \leqslant N-1)$:

$$G_N \equiv G(a_N) = N - 6 - \sum_{i=n+1}^{N-1} G_i. \tag{26}$$

Inserting a_N thus (implicitly) determined into equation (24), we obtain

$$2\bar{P} = \sum_{i=n+1}^{N-1} \lambda_i H_i + \lambda_N H_N(a_N(a_{n+1}, a_{n+2}, \ldots, a_{N-1})) + e_N \langle a \rangle \tag{27}$$

which is a function of $a_{n+1}, \ldots, a_{N-1}$. The last term in equation (27) is a constant for given N and $f(a)$. Minimization of the perimeter is effected by setting

$$2\frac{\partial \bar{P}}{\partial a_i} = \lambda_i \frac{\mathrm{d}H_i}{\mathrm{d}a_i} + \lambda_N \frac{\partial H_N}{\partial a_i} = 0 \qquad (i = n+1, \ldots, N-1) \tag{28}$$

where we have used the fact that H_i depends only on a_i (and not on the other a_k, $k \neq i$). Now, from equation (18),

$$\frac{\mathrm{d}H_i}{\mathrm{d}a_i} = a_i f(a_i) \qquad (i = n+1, \ldots, N-1) \tag{29}$$

$$\frac{\partial H_N}{\partial a_i} = \frac{\mathrm{d}H_N}{\mathrm{d}a_N}\frac{\partial a_N}{\partial a_i} = a_N f(a_N)\frac{\partial a_N}{\partial a_i}. \tag{30}$$

As noted above, equation (26) defines a_N as an implicit function of $a_{n+1}, \ldots, a_{N-1}$, whence

$$\frac{\partial a_N}{\partial a_i} = -\frac{\partial G_N/\partial a_i}{\partial G_N/\partial a_N} = -\frac{f(a_i)}{f(a_N)}. \tag{31}$$

Equation (28) becomes, upon insertion of equations (29)–(31),

$$2\frac{\partial \bar{P}}{\partial a_i} = (\lambda_i a_i - \lambda_N a_N) f(a_i) = 0 \qquad (i = n+1, \ldots, N-1). \tag{32}$$

The minimum is thus achieved for

$$a_i = \frac{\lambda_N}{\lambda_i} a_N \equiv \frac{k}{\lambda_i} \qquad (i = n+1, \ldots, N-1) \tag{33}$$

a remarkably simple result; k is a constant to be determined.

We assumed at the start that $a_{i+1} > a_i$, hence λ_i must decrease with increasing i. This is indeed the case for regular bubbles, as will be further discussed below. To find k we insert equation (33) into equation (23):

$$\sum_{i=n+1}^{N} G_i\left(\frac{k}{\lambda_i}\right) = N - 6 \tag{34}$$

where we have defined $G_i(k/\lambda_i) \equiv G_i(a_i = k/\lambda_i)$; this equation can be solved for k.

An admissible solution for the minimum perimeter requires that equation (34) has a positive solution and $a_n < k/\lambda_{n+1}$ and $a_{N+1} > k/\lambda_N$. The latter conditions are met when $a_n = 0$ and $a_{N+1} = \infty$. However, there may be distributions $f(a)$ for which there is no solution; in such cases, the smallest $\bar{P}$ is not a proper minimum.

4. Results

We approximate e_i by Graner *et al*'s result for regular Plateau cells [37]:

$$e_i = \frac{2\alpha\sqrt{i}}{\sqrt{\alpha - \frac{\sin\alpha \sin\frac{\pi}{6}}{\sin\frac{\pi}{i}}}} \qquad \alpha = \pi\left(\frac{1}{i} - \frac{1}{6}\right). \tag{35}$$

In figure 2 we plot e_i, λ_i and $1/\lambda_i$ for regular cells (from equation (35)).

The following distributions $f(a)$ of $a = \sqrt{A}$ have been considered:

1. Linear distribution: $f(a) = \epsilon + 2(1-\epsilon)a$ for $a \in [0, 1]$ $(0 \leqslant \epsilon \leqslant 2)$. If $\epsilon = 1$ this reduces to the uniform distribution, $f(a) = 1$.

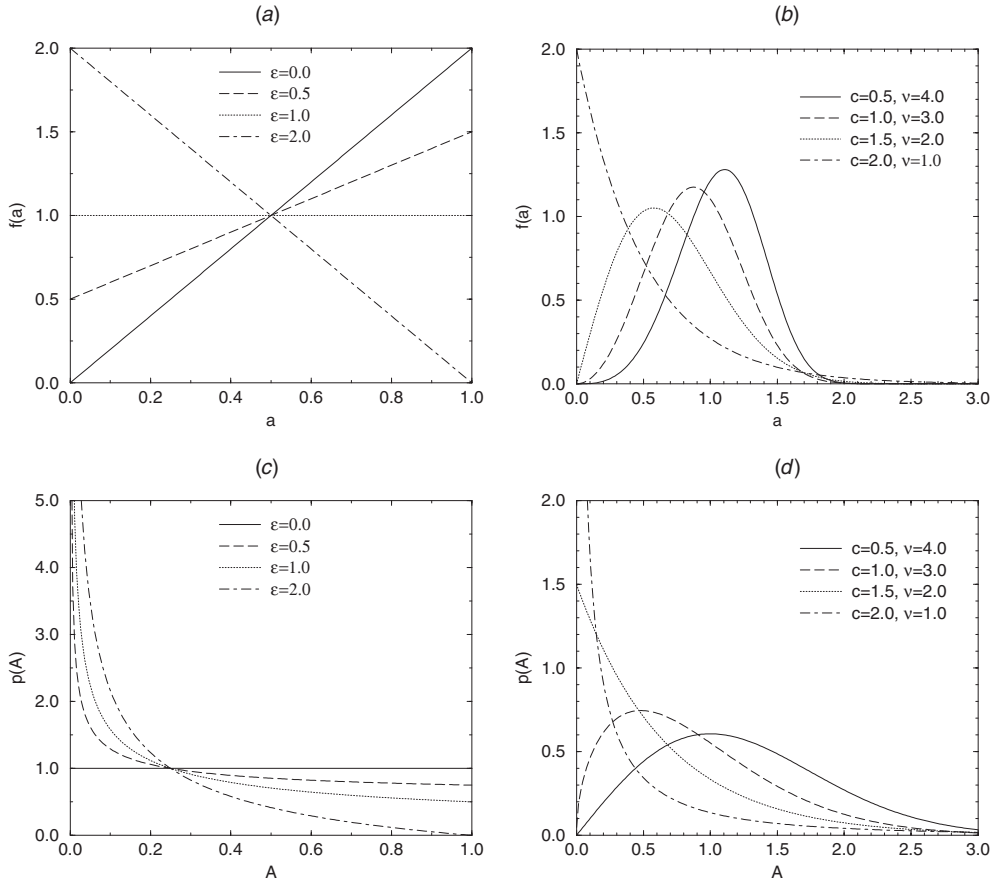

Figure 3. Examples of distributions used in the calculation of $\bar{P}_{\min}$: (*a*) linear distribution $f(a)$ of $a \equiv \sqrt{A}$ for different values of ϵ; (*b*) Weibull distribution $f(a)$ of a for different combinations of c and ν; (*c*) distribution $p(A)$ of A corresponding to the linear distribution $f(a)$ of a in (*a*); (*d*) distribution $p(A)$ of A corresponding to the Weibull distribution $f(a)$ of a in (*b*).

2. Weibull distribution [36]: $f(a) = \kappa \nu a^{\nu-1} \exp(-\kappa a^{\nu})$ for $a \in [0, \infty)$ ($\kappa, \nu > 0$). If $\nu = 1.0$ this reduces to the (pure) exponential distribution; it was chosen for its ability to reproduce realistic shapes for appropriate choices of κ and ν.

Example distributions of both types are plotted in figure 3, together with the corresponding area distributions $p(A)$ (related by equations (3)). We have also used a cubic polynomial distribution of $a \in [0, 1]$ but do not present those results here.

For each of these distributions and a choice of (n, N), k is calculated from equation (34); then a_i from equation (33); finally, the minimum perimeter per bubble, $\bar{P}_{\min}$, is obtained from equation (24), and x_i, $\langle A \rangle_i$ and $\langle P \rangle_i$ from equations (4), (7) and (8), respectively. Details of these calculations are given in the appendix. Values of $2\bar{P}_{\min}/\langle a \rangle$ for the linear and Weibull distributions of a are collected in tables 1 and 2, respectively.

For the linear distribution, we have found that $\bar{P}$ cannot be minimized for arbitrary (n, N). For example, for $\epsilon = 1.0$ (uniform distribution of a) and $n = 3$, there is no minimum if $N > 8$: the solution of equation (34) for k leads to $a_8 > 1$. On the other hand, for $\epsilon = 2.0$ and $n = 3$, equation (34) has no real roots. This appears to be a consequence of the fact that the minimum

Table 1. Minimum perimeter $2\bar{P}_{\min}/\langle a\rangle$ of films in a foam with a linear distribution of the linear bubble size $a \equiv \sqrt{A}$. A dash entry means there is no minimum of $\bar{P}$.

		$2\bar{P}_{\min}/\langle a\rangle$			
n	N	$\epsilon = 0.0$	$\epsilon = 0.5$	$\epsilon = 1.0$	$\epsilon = 2.0$
3	7	3.722 026	3.721 636	3.721 368	3.721 186
3	8	–	3.721 630	3.721 278	3.720 936
3	9	–	–	–	3.720 905
3	10	–	–	–	3.720 903
3	11	–	–	–	–
4	7	3.722 041	3.721 701	3.721 444	3.721 257
4	8	–	3.721 699	3.721 385	3.721 051
4	9	–	–	–	3.721 032
4	10	–	–	–	3.721 032
4	11	–	–	–	–
5	7	3.722 113	3.721 875	3.721 660	3.721 462
5	8	–	–	3.721 651	3.721 361
5	9	–	–	–	3.721 357
5	10	–	–	–	–
5	11	–	–	–	–

Table 2. Minimum perimeter $2\bar{P}_{\min}/\langle a\rangle$ of films in a foam with a Weibull distribution of the linear bubble size $a \equiv \sqrt{A}$. Now there is a minimum for every (n, N).

		$2\bar{P}_{\min}/\langle a\rangle$	
n	N	$\kappa = 1.0, \nu = 3.0$	$\kappa = 1.5, \nu = 2.0$
3	7	3.722 076	3.721 742
3	8	3.722 071	3.721 678
3	9	3.722 071	3.721 673
3	10	3.722 071	3.721 673
3	11	3.722 071	3.721 673
3	12	3.722 071	3.721 673
4	7	3.722 079	3.721 760
4	8	3.722 074	3.721 700
4	9	3.722 074	3.721 696
4	10	3.722 074	3.721 695
4	11	3.722 074	3.721 695
4	12	3.722 074	3.721 695
5	7	3.722 113	3.721 848
5	8	3.722 109	3.721 808
5	9	3.722 109	3.721 806
5	10	3.722 109	3.721 806
5	11	3.722 109	3.721 806
5	12	3.722 109	3.721 806

condition for $\bar{P}$ cannot be met for all (n, N) if the range of a is bounded. The same is true of the cubic polynomial distribution.

Table 1 and figure 4 show illustrative results for the linear distribution. In general, the distributions x_i of i-sided bubbles are very different from those obtained experimentally, which have a maximum around $i = 6$. The plots of $\langle A\rangle_i$ and $\langle P\rangle_i$ exhibit large deviations from linearity, although their (mostly) upward concave shape agrees with experiment [6].

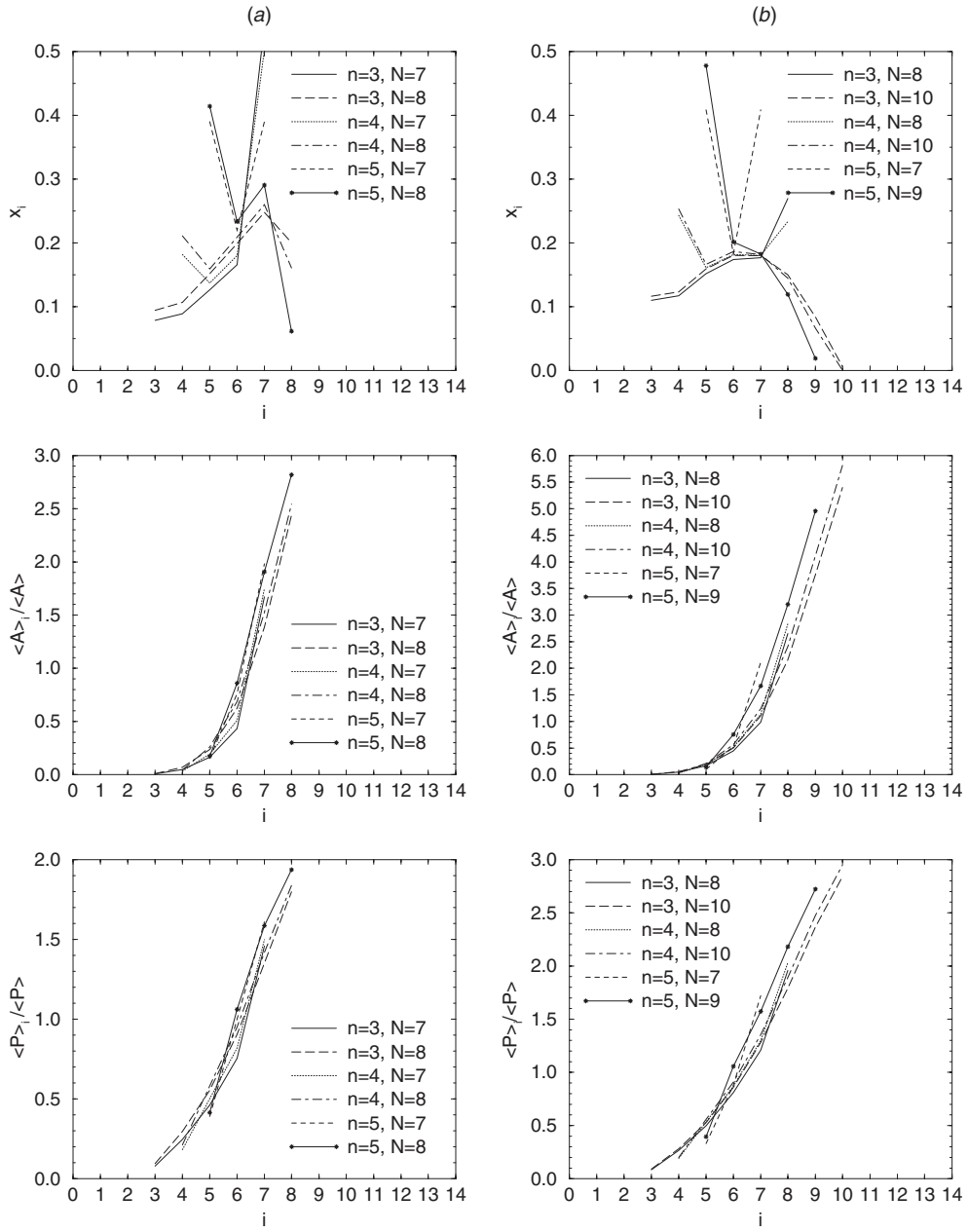

Figure 4. From top to bottom: x_i, $\langle A\rangle_i/\langle A\rangle$ and $\langle P\rangle_i/\langle P\rangle$ versus i for minimum-perimeter arrangements of bubbles with a linear distribution of $a \equiv \sqrt{A}$, for: (*a*) $\epsilon = 1.0$ (uniform distribution); and (*b*) $\epsilon = 2.0$. The slopes of the straightest (large i) portions of the $\langle A\rangle_i/\langle A\rangle$ and $\langle P\rangle_i/\langle P\rangle$ versus i curves are in the ranges 0.9–1.6 and 0.5–0.6, respectively.

Results for the Weibull distribution of a, which is of the type found in experiments, are more interesting. Now $\bar{P}$ has a minimum for any choice of (n, N), see table 2, and the x_i versus i curves have the right inverted V shape for $n = 3$ or 4, see figure 5. Curiously, for large N, typically $N \geqslant 11$ or 12, there are virtually no bubbles with $i \geqslant 10$, i.e. x_i drops below

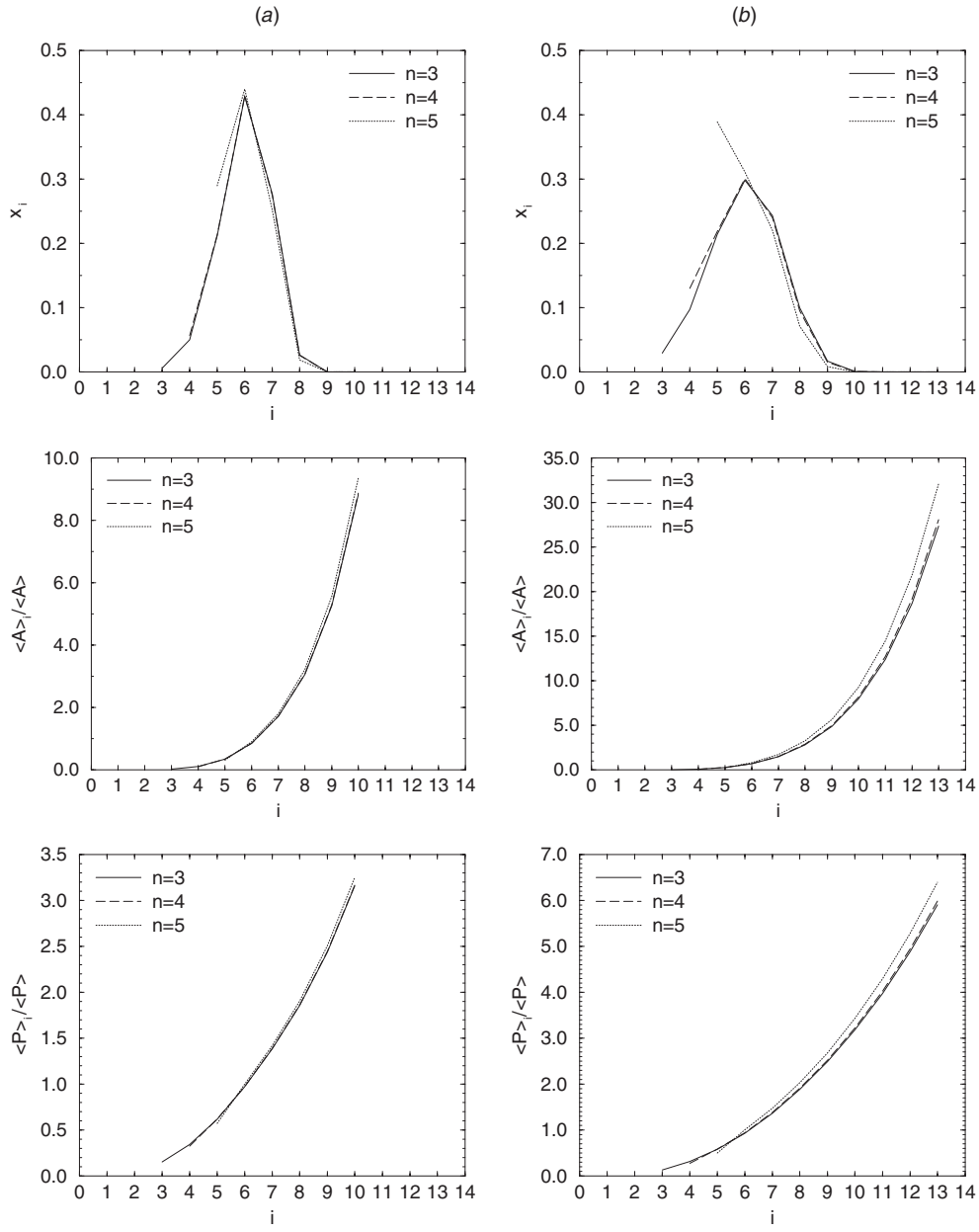

Figure 5. Same as in figure 4, but for cells with a Weibull distribution of $a \equiv \sqrt{A}$, for (*a*) $\kappa = 1.0$, $\nu = 3.0$; (*b*) $\kappa = 1.5$, $\nu = 2.0$. The effect of changing N is negligible on the scale of the plots. The slopes of the straightest (large i) portions of the $\langle A\rangle_i/\langle A\rangle$ and $\langle P\rangle_i/\langle P\rangle$ versus i curves are in the ranges 2.3–6.8 and 0.5–0.8, respectively.

machine precision for $i \geqslant 10$. This is in line with what is observed in real foams, where no bubbles with more than ∼10 sides are found. $\langle A\rangle_i$ and $\langle P\rangle_i$ are similar to those obtained for the linear distribution: again they deviate considerably from linearity, yet agree reasonably well with experiment.

For both distributions (linear and Weibull), $\bar{P}_{\min}$ decreases as N increases at fixed n, and increases as n increases at fixed N. In all cases, $\bar{P}_{\min}$ is below its value for a foam consisting exclusively of regular hexagonal bubbles. This implies that it is a minimum, rather than a maximum, of $\bar{P}$. When there is no solution of the minimization equation (28), there must nevertheless be a choice of a_i that gives the smallest $\bar{P}$ for given (n, N); we have not attempted to find it.

5. Discussion

We have shown how, given the distribution of bubble areas in a foam, it is possible to obtain the distribution of the number of bubble sides x_i, as well as average quantities such as the average area $\langle A\rangle_i$ and average perimeter $\langle P\rangle_i$ of i-sided bubbles. We have, however, been forced to make a number of simplifications. Firstly, we assumed that j-sided bubbles always have smaller area than k-sided bubbles if $j < k$. Secondly, we employed an approximate relation between $\langle P\rangle_i$ and $\langle\sqrt{A}\rangle_i$, equation (8), with e_i (weakly) dependent only on i and such that λ_i given by equation (25) is positive and a decreasing function of i. Finally, we took for e_i their values for regular bubbles, equation (35), which satisfy the above requisites. In disordered foams, however, bubbles are not in general regular, and a more appropriate choice of e_i would be $e_i = \langle P/\sqrt{A}\rangle_i$, for which no reliable expression exists. Graner *et al* [37] have argued that in a foam close to its minimum energy geometry, the perimeter of films at fixed bubble areas should not deviate too much from its value for regular bubbles: indeed, our values of $2\bar{P}_{\min}/\langle\sqrt{A}\rangle$ are all very close to that proposed by Graner, $2^{3/2}3^{1/4} \approx 3.722\,419$ [37]. Nonetheless, small changes in e_i may lead to large changes in λ_i, which in turn may significantly alter the final partitioning of bubble sizes and numbers of sides.

In spite of the above simplifications, results obtained for x_i, $\langle A\rangle_i$ and $\langle P\rangle_i$ using the more realistic Weibull distribution of bubble areas agree qualitatively with experiment. The plots of $\langle A\rangle_i$ and $\langle P\rangle_i$ versus i are, however, clearly not linear, as indeed is experimentally observed. For this distribution, with a unbounded above, the energy/perimeter could be minimized for any n and N, the minimum and maximum number of bubble sides, respectively.

A linear distribution of a yields x_i very different from experiment, although $\langle A\rangle_i$ and $\langle P\rangle_i$ are still reasonable. For this and for a cubic polynomial distribution, both defined in a bounded range of a, there are (n, N) pairs for which $\bar{P}$ does not have a minimum.

Acknowledgment

PICT acknowledges partial funding from the Fundação para a Ciência e Tecnologia (Portugal).

Appendix. Calculational details

A.1. Linear distribution

For $f(a) = \epsilon + 2(1-\epsilon)a$ $(0 \leqslant \epsilon \leqslant 2)$ we have:

$$G(a) = \epsilon a + (1-\epsilon)a^2 \tag{A1}$$

$$H(a) = \frac{\epsilon}{2}a^2 + \frac{2}{3}(1-\epsilon)a^3. \tag{A2}$$

k in equation (33) is the smaller real and positive root of the quadratic equation

$$(1-\epsilon)\mathcal{C}k^2 + \epsilon\mathcal{B}k - (N-6) = 0 \tag{A3}$$

where

$$\mathcal{B} = \sum_{i=n+1}^{N} \frac{1}{\lambda_i} \qquad \mathcal{C} = \sum_{i=n+1}^{N} \frac{1}{\lambda_i^2}. \tag{A4}$$

(In case there are two real roots, we have checked that it is the smaller one that gives the lowest $\bar{P}_{\min}$.) For the minimum perimeter $\bar{P}_{\min}$, equation (24) yields

$$2\bar{P}_{\min} = \frac{2}{3}(1-\epsilon)\mathcal{C}k^3 + \frac{\epsilon}{2}\mathcal{B}k^2 + e_N\left(\frac{2}{3} - \frac{\epsilon}{6}\right) \tag{A5}$$

with k given by equation (A3). x_i, $\langle A\rangle_i$ and $\langle P\rangle_i$ follow from equations (4), (6), (7) and (8), and have fairly simple analytical expressions.

A.2. Weibull distribution

For $f(a) = \kappa\nu a^{\nu-1}\exp(-\kappa a^{\nu})$ ($\kappa, \nu > 0$) we have:

$$G(a) = 1 - \exp(-\kappa a^{\nu}). \tag{A6}$$

There is no analytical expression for $H(a)$. Equation (33) for k was solved using NETLIB routine HYBRD [39]. Then the integrals in equations (4), (6), (7) for x_i, $\langle a\rangle_i$ and $\langle A\rangle_i$ were performed by Romberg quadrature [38].

References

[1] Lewis F T 1928 *Anat. Rec.* **38** 341
[2] Lewis F T 1931 *Anat. Rec.* **50** 235
[3] Lewis F T 1943 *Am. J. Bot.* **30** 766
[4] Lewis F T 1944 *Am. J. Bot.* **31** 619
[5] Weaire D and Rivier N 1984 *Contemp. Phys.* **25** 59
[6] Glazier J A, Gross S P and Stavans J 1987 *Phys. Rev.* A **36** 306
[7] Stavans J, Domany E and Mukamel D 1991 *Europhys. Lett.* **15** 479
[8] Szeto K Y and Tam W Y 1995 *Physica* A **221** 256
[9] Fradkov V E, Shvindlerman L S and Udler D G 1985 *Scr. Metall.* **19** 1285
[10] Fradkov V E, Kravchenko A S and Shvindlerman L S 1985 *Scr. Metall.* **19** 1291
[11] Ciupiński L, Kurzydłowski K J and Ralph B 1998 *Mater. Charact.* **40** 215
[12] Pereira H, Rosa M E and Fortes M A 1987 *IAWA Bull.* **8** 213
[13] Mombach J C M, Vasconcellos M A Z and Almeida R M C 1990 *J. Phys. D: Appl. Phys.* **23** 600
[14] Pina P and Fortes M A 1996 *J Phys. D: Appl. Phys.* **29** 2507
[15] Lemaître J, Gervois A, Troadec J P, Rivier N, Ammi M, Oger L and Bideau D 1993 *Phil. Mag.* B **67** 347
[16] Annic C, Troadec J P, Gervois A, Lemaître J, Ammi M and Oger L 1994 *J. Physique* I **4** 115
[17] Noever D A 1991 *Phys. Rev.* A **44** 968
[18] Noever D A 1992 *Langmuir* **8** 1036
[19] Noever D A 1994 *J. Mat. Res.* **9** 515
[20] Cerisier P, Rahal S and Rivier N 1996 *Phys. Rev.* E **54** 5086
[21] Fortes M A 1995 *J. Phys. A: Math. Gen.* **28** 1055
[22] Desch C H 1919 *J. Inst. Met.* **22** 241
[23] Rivier N 1985 *Phil. Mag.* B **52** 795
[24] Feltham P 1957 *Acta Metall.* **5** 97
[25] Kornetta W, Mendiratta S K and Menteiro J 1998 *Phys. Rev.* E **57** 3142
[26] Noever D A 1994 *Astrophys. Space Sci.* **220** 65
[27] Noever D A 1995 *J. Coll. Int. Sci.* **174** 92
[28] Rivier N and Lissowski A 1982 *J. Phys. A: Math. Gen.* **15** L143
[29] Chiu S N 1995 *J. Phys. A: Math. Gen.* **28** 607
[30] Mulheran P A 1992 *Phil. Mag. Lett.* **66** 219
[31] Hinrichsen H and Schliecker G 1998 *J. Phys. A: Math. Gen.* **31** L451
[32] Flyvbjerg H 1993 *Phys. Rev.* E **47** 4037

[33] Aboav D 1970 *Metallography* **3** 383
[34] Weaire D 1974 *Metallography* **7** 157
[35] Aboav D 1980 *Metallography* **13** 43
[36] Weibull W 1951 *J. Appl. Mech.—Trans. ASME* **18** 293
[37] Graner F, Jiang Y, Janiaud E and Flament C 2001 *Phys. Rev.* E **63** 011402
[38] Press W H, Teukolsky S A, Vetterling W T and Flannery B P 1992 *Numerical Recipes: the Art of Scientific Computing* 2nd edn (Cambridge: Cambridge University Press)
[39] Webpage http://www.netlib.org/minpack/hybrd.f